

GRB Light Curves in the Relativistic Turbulence and Relativistic Sub-Jets Models

Ayah Lazar^{1,2}, Ehud Nakar^{3,4} and Tsvi Piran¹

1. The Racah Institute of Physics, Hebrew University, Jerusalem 91904, Israel

2. Department of Geophysics and Planetary Sciences, Tel Aviv University, Tel Aviv 69978 Israel

3. Raymond and Beverly Sackler School of Physics & Astronomy, Tel Aviv University, Tel Aviv 69978, Israel

4. Theoretical Astrophysics, Caltech, Pasadena, CA 91125, USA

ABSTRACT

Randomly oriented relativistic emitters in a relativistically expanding shell provides an alternative to internal shocks as a mechanism for producing GRBs' variable light curves with efficient conversion of energy to radiation. In this model the relativistic outflow is broken into small emitters moving relativistically in the outflow's rest frame. Variability arises because an observer sees an emitter only when its velocity points towards him so that only a small fraction of the emitters are seen by a given observer. Models with significant relativistic random motions require converting and maintaining a large fraction of the overall energy into these motions. While it is not clear how this is achieved, we explore here, using two toy models, the constraints on parameters required to produce light curves comparable to the observations. We find that a tight relation between the size of the emitters and the bulk and random Lorentz factors is needed and that the random Lorentz factor determines the variability. While both models successfully produce the observed variability there are several inconsistencies with other properties of the light curves. Most of which, but not all, might be resolved if the central engine is active for a long time producing a number of shells, resembling to some extent the internal shocks model.

Subject headings: gamma-rays: bursts; turbulence;

1. Introduction

GRB's temporal variability played a major role in the understanding how GRBs operate. Standard external shocks, in which the external medium slows the relativistic ejecta, cannot produce efficiently variable light curves (Sari & Piran 1997). While internal shocks resolve the variability and agree with other properties of GRB light curves (e.g. Nakar & Piran 2002b; Ramirez-Ruiz & Fenimore 2000) they suffers from several drawbacks. First and foremost is their low efficiency (Kobayashi et al. 1997; Daigne & Mochkovitch 1998 see however, Kobayashi et al. 1997; Kobayashi & Sari 2001; Beloborodov 2000). This is particularly troublesome in view of the high efficiency implied from comparison of the prompt γ -rays luminosity and the kinetic energy that remains in the outflow. Detailed models for the emission mechanisms of the prompt γ -rays pose other problems (Kumar & McMahon 2008).

External shocks can produce highly variable light curves if the outflow is slowed down by small external clumps. Each clump producing a short pulse. However, this process will inevitably be inefficient (Sari & Piran 1997) as the overall covering factor of the emitting regions is $\delta t/T$ (δt and T are the pulses' and the burst's durations). Observed values of $\delta t/T$ are typically ~ 0.01 and in can be as low as 10^{-4} (Nakar & Piran 2002a).

Lyutikov & Blandford (2002, 2003) (see also Lazar 2005 [L05], Lyutikov 2006, Narayan & Kumar 2008) proposed that variability can be recovered while maintaining high efficiency if the shell that moves with a bulk Lorentz factor Γ contains emitting clumps (see fig. 1) that move with random macroscopic relativistic velocities (with a Lorentz factor γ'). A clump is observed only when its radiation cone (with an opening angle of the order of $1/\Gamma\gamma'$ in the lab frame) points towards the observer. The filling factor of the clumps may be unity, recovering high efficiency. However, as only a small fraction of the clumps are observed at any given time, the light curve can show rapid variability. The overall duration of the burst, is the larger between the angular time and the shell's light crossing time ($\max\{R/c\Gamma^2, \Delta/c\}$), where R and Δ are the shell's radius and width respectively and c is the light speed, allowing for emission radii much larger than $\delta t\Gamma^2$, required in the internal shocks model. The temporal variability is then dictated by the random Lorentz factor, γ' , reflecting the activity of the emitting region and not those of the inner engine.

While it is unclear how macroscopic random relativistic motion can be generated, we assume that it does and examine, using two simplified toy models that includes the essential ingredients, the conditions under which the temporal features of the observed light curve can be produced (see L05). We describe our first toy model, which we call here relativistic turbulence, and derive analytic constraints and numerical light curves in §2. In §3 we consider a second toy model proposed by Lyutikov (2006) that is based on sub-jets and compare it with the first one. We summarize the results and compare both models with observations in §4.

2. Relativistic Turbulence

Our (L05) kinematic toy model for relativistic turbulence considers a shell which is divided into discrete randomly distributed emitters that have randomly oriented relativistic velocities. The emitters change their direction of motion continuously, as expected in a turbulent medium. Since the emitters exhibit a coherent macroscopic motion, we require that each emitter is causally connected, and that it changes its direction on times longer than the causal time scale but shorter than the shell crossing time. The length scale of the emitter in its own rest frame, l'' , is assumed to be similar in all three dimensions, and it emits isotropically in this frame. We define a dimensionless scale $\psi \equiv l''/R$, which is the angular scale of an emitter that points towards the observer (see inset of fig 1). The emitters radiate as the shell moves from R_0 to $2R_0$. Due to the turbulent motion the positions and directions of the emitters change with time. We model this by a set of successive shells between R_0 and $2R_0$. Each new shell is constructed with randomly distributed emitters, representing the random changes in direction of the turbulent motion. The time difference between two shells is, τ' , the time it takes for the emitters to turn an angle of γ'^{-1} (in the shell frame).

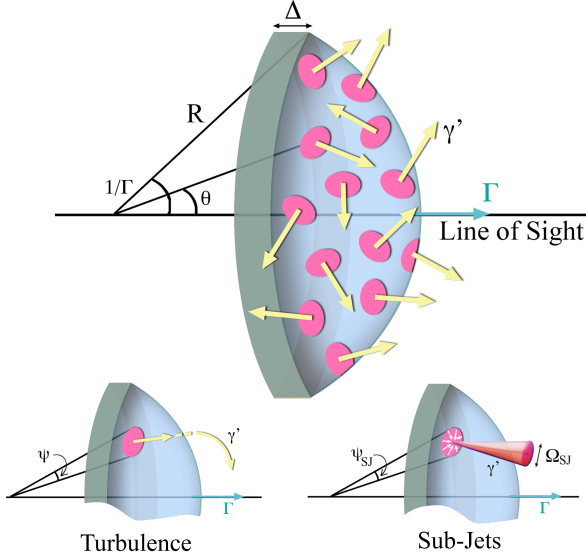


Fig. 1.— The basic kinematic model – relativistically expanding shell with an ensemble of emitters, which are moving at random relativistic velocities within the shell. The inserts describe the geometrical details and definitions of the two alternative models. Left: relativistic turbulence - emitters of size $R\psi$ move relativistically; Right: sub-jets - energy from regions of size $R\psi_{SJ}$ is extracted into relativistic jets.

Note that there are three frames: The lab frame; the shell's frame, denoted by a prime, which is boosted radially with a Lorentz factor Γ relative to the lab; and the frame of each emitter, denoted by two primes, which is boosted by (randomly oriented) γ' relative to the shell frame. The observer is, of course, at rest relative to the lab frame. However, the observer time, namely the arrival time of photons (denoted t) differs from the lab time by the usual time of flight arguments (Rybicki & Lightman 1979).

The Doppler shift from an emitter is:

$$\Lambda = [\gamma(1 - \beta \cdot \cos \alpha)]^{-1}, \quad (1)$$

where γ , β and α are the Lorentz factor, velocity and the angle between the velocity and the line to the observer (both in the lab frame). The flux that reaches the observer from this emitter is:

$$F_\nu = \int I''_{\nu''} \Lambda^3 d\Omega_i \approx I''_{\nu''} \Lambda^3 \frac{\psi^2 R^2}{D^2}, \quad (2)$$

where $I''_{\nu''}$ is the specific intensity and the second relation holds for a small enough emitter (D is the distance to the observer). An implicit K correction arises from the difference between the ν and ν'' .

Define θ as the angle between the line that connects the origin and the emitter and the line that connects the origin and the observer (see inset of fig 1). The maximal Doppler boost, $\Lambda_{max} = 4\gamma'\Gamma$, is obtained for emitter at $\theta = 0$ that moves along the line of sight. The flux decreases like Λ^3 plus a K correction. Therefore, we consider emitters only if $\Lambda_i > \Lambda_{max}/2$. What is then the probability that an emitter at angle

θ is observed, $dP/d\theta \equiv S(\theta, \Gamma, \gamma')$? At $\theta = 0$ it is $S(0, \Gamma, \gamma') \approx 1/4\gamma'^2$ while $S(1/\Gamma, \Gamma, \gamma') = 0$. This suggests that S scales as $S(\theta, \Gamma, \gamma') = \gamma'^{-2} \tilde{S}(\theta\Gamma)$ (L05), implying that the average probability that an emitter will be visible from an arbitrary position on the shell is:

$$P(\Gamma, \gamma') \approx \frac{1}{2(\Gamma\gamma')^2} \int_0^1 \tilde{S}(\theta\Gamma)(\theta\Gamma)d(\theta\Gamma) \approx \frac{0.3}{4\pi(\Gamma\gamma')^2}. \quad (3)$$

The factor 0.3 was evaluated numerically (L05) and can be ignored at the accuracy level of our discussion.

The arrival time from an emitter at R, θ is:

$$T = \frac{R - R_0}{2c\Gamma^2} + \frac{R\theta^2}{2c} + \frac{x}{c}, \quad (4)$$

where $x(< \Delta)$ is the distance of the emitter from the front of the shell. As the last photons will arrive from $2R_0$, an angle of $1/\Gamma$ and $x = \Delta$, the overall duration of the burst will be a function only of Δ and Γ (and not γ'):

$$T \approx \frac{R_0 d}{c\Gamma^2}. \quad (5)$$

where we define $d \equiv \Delta\Gamma^2/R$. As the shell is expected to expand relativistically in its own frame¹ $d \gtrsim 1$. For $d > 1$ the shell's width, as well as T , are determined by the engine activity time while for $d = 1$ they don't.

The duration of a pulse arriving from a single emitter is the longest of the three following time scales:

(i) The duration over which the emitter points towards the observer, namely the duration over which the direction of motion varies by an angle $1/\Gamma\gamma'$ in the lab frame ($1/\gamma'$ in the shell's frame). As the emitter is confined to the shell it should make at least a $\pi/2$ turn during Δ'/c , implying that the time to turn by $1/\gamma'$ (shell's frame), τ' , is shorter than $\Delta'/c\gamma'$. Causality puts a lower limit on τ' of $R\psi/c$. Therefore:

$$R\psi/c \leq \tau' \leq \Delta'/c\gamma'. \quad (6)$$

In the observer's frame, this translates to:

$$R\psi/\Gamma\gamma'^2 c \leq \tau \leq \Delta/c\gamma'^3. \quad (7)$$

(ii) The emitter's light crossing time in the lab frame (in the direction along the line of sight). For an emitter moving towards the observer this time is $R\psi/\gamma'\Gamma$. (iii) The angular time scale – At the largest possible angle, where the emitter is still visible by the observer, $1/\gamma'\Gamma$, the time difference between the first and the last photon would be $\frac{1}{c}R\psi \sin(1/\gamma'\Gamma) \approx R\psi/c\gamma'\Gamma$. Overall (ii) and

(iii) are of the same order and much larger than (i). Thus:

$$\delta t \approx R\psi/c\gamma'\Gamma. \quad (8)$$

¹Note that for a hydrodynamic external shock $d \lesssim 1$ Sari & Piran (1997) but this might not be relevant here.

Using Eqs. 5 and 8 we express, N_p , the number of (possibly overlapping) pulses expected in a burst:

$$N_p \equiv n_p \frac{T}{\delta t} = n_p \frac{d\gamma'}{\psi\Gamma} \quad (9)$$

where n_p is the occupation number of pulses at any given observer time (i.e., $n_p \gg 1$ implies many overlapping pulses while $n_p \ll 1$ implies long quiescent periods between isolated pulses).

The number of emitters is $4\pi R^2 \Delta' / (R\psi)^3 = 4\pi \Delta\Gamma / R\psi^3$. The emitters obtain new random directions (which differ by more than $1/\gamma'$, in the shell's frame, than the previous ones) after a time τ' . Thus, the total number of independent emitters, N_{tot} , is larger by the factor $R/(c\Gamma\tau')$, the ratio of the total duration over which the radius doubles and τ' . Finally we introduce a filling factor $f \leq 1$ allowing for the possibility that not all emitters are active all the time or that space is not fully covered by emitters ($f \ll 1$ is strongly disfavored as the efficiency is always smaller than f). Overall we find:

$$N_{tot} = \frac{4\pi f}{\psi^3} \frac{d}{\Gamma^2} \frac{R}{c\tau'}. \quad (10)$$

The condition $N_p = PN_{tot}$ yields:

$$n_p = \frac{fd}{\gamma'^3 \Gamma^3 \psi^2} \frac{R}{c\tau'}, \quad (11)$$

and using 7:

$$\frac{f}{d(\gamma'\Gamma\psi)^2} \leq n_p \leq \frac{f}{(\gamma'\Gamma\psi)^3}. \quad (12)$$

We demand $n_p \approx 1$ since many overlapping pulses reduce the observed variability, whereas very frequent long quiescent times between pulses are not observed. If the shell is in the freely expanding phase (i.e., $d \approx 1$) n_p will be of order unity if:

$$\psi \approx f^{1/k} \frac{1}{\gamma'\Gamma}, \quad (13)$$

where k is between 2 and 3. Narayan & Kumar (2008) have pointed out that $\psi = 1/\gamma'\Gamma$ if one requires that the emitters are of the maximal causally allowed size. Note that n_p depends quite sensitively on $\gamma'\Gamma\psi$ and it increases rapidly if ψ is smaller than $1/\gamma'\Gamma$. This implies, for example, that a significant number of small eddies, which may arise in a turbulent cascade, may be problematic. Using the relations 13 and 9, and assuming the causal limit for τ' :

$$\gamma' \approx \left(\frac{f}{n_p}\right)^{1/6} \sqrt{\frac{T}{d\delta t}}, \quad (14)$$

leading to $\gamma' \approx 10/\sqrt{d}$ for typical values of $T/\delta t$. Note that while the model determines γ' it does not constrain Γ and R .

Fig. 2 depicts simulated light curves (L05) for four choices of parameters. The two upper panels have $n_p = 1$ with different emitter sizes. Both light curves are highly variable and densely filled with non-overlapping pulses. However, as $d = 1$, the underlying overall envelope of the pulses is seen. As the emitters are smaller on the right panel it has more pulses than the left one. The envelope is observed since only a

small fraction of the volume and hence fewer pulses are seen early on. Similarly at $t > (d + 1)R_0/2c\Gamma^2$ pulses from small θ values are not seen, implying that only lower amplitude pulses (on average) are observed during the last $T/(d + 1)$ of the burst. The envelope is stretched on bottom panels where $d = 10$. The lower left panel depicts a very low n_p with a rather sparse light curve. The lower right panel depicts a light curve of a wide shell and $n_p = 0.7$, which is rather similar to observed bursts. For $n_p \gg 1$ (not shown) the pulses are overlapping and all variability is erased, leaving only the envelope.

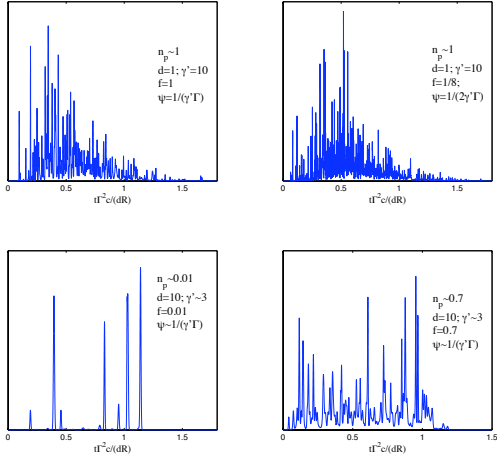


Fig. 2.— Numerical monte Carlo simulations of light curves for different combinations of parameters (shown on each frame; the scalings used eliminate the dependence on R and Γ). The flux of each pulse is calculated assuming that the radiation efficiency is constant per unit mass for all emitters in their rest frame, namely that $I''_{\nu''} \propto (\psi R)^{-3}$, therefore $F_\nu \propto \Lambda^3/(\psi R)$. We approximate each pulse as a Gaussian with the above parameters and we sum over all contributions to construct a light curve. In both upper frames $n_p = 1$ and $d = 1$. In the top left, the emitters are as large as causality allows while on the top right they are 1/2 of this value and the filling factor is lowered to compensate. In both the overall envelope is seen clearly. The sparsity of pulses is apparent when $n_p = 0.01$ (bottom left) and the "straightening out" of the envelope is clearly seen (bottom two panels) when $d = 10$.

3. Relativistic Sub-Jets

Motivated by reconnection in highly magnetized outflow Lyutikov (2006) considers a model in which relativistic sub-jets (SJs) are accelerated to a Lorentz factor γ' by dissipation of the bulk energy in many different "mini-engines" within the relativistically expanding shell. These "mini-engines" or acceleration sites correspond to reconnection sites within the magnetized flow (e.g., Lyutikov & Blackman 2001). The "mini-engines" are at rest in the shell frame. Each mini-engine operates for a time t'_{SJ} . The directions of the accelerated sub-jets are random in the shell frame but the opening angle and direction of each is constant while its mini-engine is active.

The sub-jet extracts energy from a region of size $l' = \delta t'_{SJ} \hat{\beta} c$, where $\hat{\beta} c$ is the speed of extraction of energy from the surrounding region (relativistic reconnection suggests $\hat{\beta} \approx 0.1$, Lyubarsky 2005). The observed duration is:

$$\delta t_{SJ} = \frac{t'_{SJ}}{\Gamma} \approx \frac{R \psi_{SJ}}{\hat{\beta} c \Gamma}, \quad (15)$$

where we define the dimensionless parameter $\psi_{SJ} \equiv l'/R$. Slightly generalizing Lyutikov (2006) we write the probability to observe an emitter as $\phi^2/4\pi\Gamma^2$, where $\phi = \max(\sqrt{\Omega_{SJ}}, 1/\gamma')$ and Ω_{SJ} is the sub-jet opening solid angle. Following the notation of §2, we define, f , the filling factor of regions from which energy is extracted into the sub-jets ($N_{tot} \equiv f4\pi\Delta'R^2/l'^3$). The occupation number of observed pulses is:

$$n_{pSJ} = \frac{f\phi^2}{\hat{\beta}\psi_{SJ}^2\Gamma^2}. \quad (16)$$

The condition $n_{pSJ} \approx 1$ yields:

$$\psi_{SJ} \approx \frac{\sqrt{f}\phi}{\hat{\beta}^{1/2}\Gamma}, \quad (17)$$

and

$$\frac{T}{\delta t} \approx \frac{\hat{\beta}^{3/2}d}{\phi\sqrt{f}} \leq \gamma' \frac{\hat{\beta}^{3/2}d}{\sqrt{f}}. \quad (18)$$

This implies that an efficient ($f \sim 1$) highly variable burst requires either a large γ' or a wide shell (for $T/\delta t \sim 100$, $\gamma'd \sim 100\hat{\beta}^{-3/2}$).

This constant direction of the emitters and the fact that causality in the shell's frame determines the sub-jet size, $c\delta t'$, are the main kinematic differences between the sub-jet and the turbulence model (in which the emitter's direction varies and causality in the emitter's frame determine its size, l''). For the same n_p and $\delta t/T$ the two models give similar light curves. In particular, an overall (rising and falling) envelope for the light curve is expected in the sub-jet model as well.

4. Discussion and Conclusions

We have derived conditions on the parameters of relativistic random emitters needed for producing variable GRB light curves. This is characterized by $n_p \approx 1$ which ensures that typical pulses don't overlap and are not too sparse either. Our numerical simulations show that for $0.03 < n_p < 3$ one obtains light curves that resemble observed GRBs (see fig. 2). The resulting light curves do not change qualitatively when we introduce a distribution of turbulent Lorentz factors and sizes.

Causality suggests, for relativistic turbulence, that the relation $\psi = 1/\Gamma\gamma'$ between the angular size of the emitters, ψ , and the turbulent and the bulk Lorentz factors holds naturally (Narayan & Kumar 2008). But, this condition holds when the turbulent eddies are of the maximal possible size and may be broken by cascade to lower scales. The condition, $\psi_{SJ} = \sqrt{f}\phi/\hat{\beta}^{3/2}\Gamma$ arises in the sub-jets model. For high efficiency, negligible sub-jet opening angle assuming $\hat{\beta} \sim 1$ this reduces to $\psi_{SJ} \sim 1/\Gamma\gamma'$ or $t'_{SJ} \approx R/c\Gamma\gamma'$. While

this is similar to the one obtained in the turbulent model, here there is no apparent physical motivation for proportionality between t'_{SJ} and $1/\gamma'$ and this requires an ad hoc fine tuning.

In both models the light curves arising from a single expanding shell with $d \approx 1$ shows a rising and falling underlying envelope. Furthermore, a single shell cannot produce bursts which depict long quiescent periods. The envelope can be erased if $d \gg 1$, while quiescent periods require an outflow of several shells (where naturally $d \gg 1$). These solutions become marginal in the turbulent model if τ' is determined by causality, since $\gamma' \gg 1$ requires $d \lesssim 10$ (see Eq. 14). The sub-jet model, however, may favor $d \gg 1$ as it reduces the required value of γ' .

It seems that with proper conditions (and rather reasonable in the case of the relativistic turbulence) these models can produce (efficiently) the observed highly variable GRB light curves. We turn now to several shortcomings. First and foremost is the question how such macroscopic relativistic motions can be generated and sustained. One needs to convert $\sim (1 - 1/\gamma')f$ of the initial total energy to the kinetic energy of the emitters and further dissipation in the emitters' frame is needed to generate the radiation. Additional questions involve the shape and other properties of individual pulses versus those seen in observed pulses:

(i) GRBs show a clear difference between the fast rise and the slow decline of individual pulses (Norris et al. 1996). The light curve of an individual pulse results from a combination of the motion of the emitter, its orientation relative to the observer, its width as well as intrinsic inhomogeneities within the emitter. In the relativistic turbulence model the emitter was radiating long before its velocity pointed towards the observer and it continues to emit long after it moves away from the observer. There is no reason (on average) for a difference between the rising and falling phases of an individual pulse². This is not a problem in the sub-jets model in which the onset of the pulse corresponds to the beginning of the activity of the emitter.

(ii) The temporal structure of the first and second halves of GRB light curves are similar (Ramirez-Ruiz & Fenimore 2000). The light curves produced in the two models have an overall envelope that favors stronger pulses earlier and weaker ones later. This might be resolved by a combination of several emitting shells or with very wide shells, but here fine tuning is required in the turbulent model in order to keep $\gamma' \gg 1$.

(iii) Weaker and denser pulses (arriving from emitters not moving directly towards the observer) continues at $t > T$ producing the typical envelope of high latitude emission (Kumar & Panaitescu 2000). This is consistent with rapid declines seen in some the early afterglows. However in many cases the decline is faster. In the internal shocks model this is attributed to the dominant contribution of a late pulse, that shifts the zero point of the time. Such an option does not arise here unless, once more, we allow for several shells or a single wide shell.

(iv) The duration of an observed pulse is correlated with the preceding interval (Nakar & Piran 2002b; Quilligan et al. 2002). There is no reason that such correlation should appear in both models.

(v) These models predict a Doppler induced correlation between the intensity and E_{peak} . While stronger peaks are typically harder, it is not clear whether this specific relationship is satisfied.

²Note that systematic variation of the emitter properties on a time scale of τ' will result in a strong signature differentiating between early and late phases of the overall light curve, which is not observed. On the other hand non-systematic variations (e.g., deceleration and acceleration) are expected to result in similar affects on the temporal structure of rising and decaying parts of pulses.

We could not find obvious modifications that will address all these issues. While it is not clear that those cannot be found, this suggests that the simple versions of these models might not be enough. A simple extension of a wide shell $d \gg 1$ or several separated shells might resolve some of the issues and it might be essential for the sub-jet model allowing moderate values of the sub-jet's Lorentz factor.

This research is supported by the ISF center of excellence in High Energy Astrophysics (TP & AL), Marie Curie IRG grant (EN), advanced ERC excellence award and the Schwartzmann chair (TP).

REFERENCES

- A.M. Beloborodov 2000, *Ap. J. Lett.*, 539, L25
- Daigne, F., & Mochkovitch, R. 1998, *MNRAS*, 296, 275
- Kobayashi, S., & Sari, R. 2001, *Ap. J.*, 551, 934
- Kobayashi, S., Piran, T., & Sari, R. 1997, *Ap. J.*, 490, 92
- Kumar, P., & Panaitescu, A. 2000, *Ap. J. Lett.*, 541, L51
- Kumar, P., & McMahon, E. 2008, *MNRAS*, 384, 33
- Lazar, A., MSc. Thesis: Kinematics of Time-Scale Variability in Gamma-Ray Bursts: The Relativistic Turbulence Model, 2005, Hebrew University denoted L05
- Lyubarsky, Y. E. 2005, *MNRAS*, 358, 113
- Lyutikov, M., & Blackman, E. G. 2001, *MNRAS*, 321, 177
- Lyutikov, M. & Blandford, R., 2002, *astro-ph/0210671*
- Lyutikov, M. & Blandford, R., 2003, *astro-ph/0312347*
- Lyutikov, M. 2006, *MNRAS*, 369, L5
- Nakar, E., & Piran, T. 2002a, *MNRAS*, 330, 920
- Nakar, E., & Piran, T. 2002b, *MNRAS*, 331, 40
- Nakar, E., & Piran, T. 2002c, *Ap. J. Lett.*, 572, L139
- Narayan, R., & Kumar, P. 2008, *arXiv:0812.0018*
- Norris, J. P., Nemiroff, R. J., Bonnell, J. T., Scargle, J. D., Kouveliotou, C., Paciesas, W. S., Meegan, C. A., & Fishman, G. J. 1996, *Ap. J.*, 459, 393
- Quilligan, F., McBreen, B., Hanlon, L., McBreen, S., Hurley, K. J., & Watson, D. 2002, *Astron. & Astrophys.*, 385, 377

Ramirez-Ruiz, E., & Fenimore, E. E. 2000, *Ap. J.* , 539, 712

Rybicki, G. B., & Lightman, A. P., 1979, John Wiley & Sons (*Radiative Processes in Astrophysics*)

Sari, R., & Piran, T. 1995, *Ap. J. Lett.*, 455, L143

Sari, R., & Piran, T. 1997, *Ap. J.* , 485, 270